Anomalous diffusion exponents in continuous two-dimensional multifractal media

Jean-Raynald de Dreuzy,[1] Philippe Davy,[1] Jocelyne Erhel,[2] and Jean de Brémond d'Ars[1]

[1]*Géosciences Rennes, UMR CNRS 6118, Université de Rennes, Campus de Beaulieu, 35042 Rennes Cedex, France*
[2]*IRISA/INRIA, Rennes, Campus de Beaulieu, 35042 Rennes cedex, France*

We study diffusion in heterogeneous multifractal continuous media that are characterized by the second-order dimension of the multifractal spectrum D_2, while the fractal dimension of order 0, D_0, is equal to the embedding Euclidean dimension 2. We find that the mean anomalous and fracton dimensions, d_w and d_s, are equal to those of homogeneous media showing that, on average, the key parameter is the fractal dimension of order 0 D_0, equal to the Euclidean dimension and not to the correlation dimension D_2. Beyond their average, the anomalous diffusion and fracton exponents, d_w and d_s, are highly variable and consistently range in the interval [1,4]. d_w can be consistently either larger or lower than 2, indicating possible subdiffusive and superdiffusive regimes. On a realization basis, we show that the exponent variability is related to the local conductivity at the medium inlet through the conductivity scaling.

I. INTRODUCTION

Diffusion in disordered media pertains to a large range of phenomena, including for example fluid flow and electrical conductivity, and has been an active field of research in the past decades [1–3]. Diffusion has been mostly studied in archetypal deterministic and random fractal media like the Sierpinski gasket [4–6], the percolation cluster at threshold [1,7], and the percolation cluster at threshold with long-range correlations [8–10]. Such fractals are discontinuous media characterized by a binary conductivity distribution: a unit homogeneous conductivity on the fractal and zero conductivity outside. Some studies have addressed the problem of fractal media having a heterogeneous distribution of conductivities on the percolation cluster near the percolation threshold [11,12]. One recent study handled diffusion in nonfractal continuous media with long-range correlations generated by a fractional Brownian motion [13]. Whatever the fractal structure, diffusion has been found to be anomalously slow [2]. The classical measure of the anomalous diffusion is the exponent d_w characterizing the evolution of the mean square radius of diffusion $\langle R^2(t)\rangle$ with the time t as: $\langle R^2(t)\rangle \sim t^{2/d_w}$. The anomalously slow diffusion is traduced by values of d_w larger than 2. Diffusion in homogeneous media is recovered for $d_w = 2$.

In this paper, we study diffusion in bidimensional continuous media having long-range correlations without limits outside the system cutoffs. Practically continuous media will be simulated by a regular square grid. The physical parameter is the conductivity K distributed over the grid. The dimension of the support is the fractal dimension of order 0, D_0, and is equal to the embedding Euclidean dimension d. The dimension of correlation of the conductivity field, equal to the second-order dimension of the multifractal spectrum D_2 [14], is lower than the Euclidean dimension and more precisely in the range $[d-1,d[$. Because the zero and second-order fractal dimensions are different, these media are multifractal. We call them continuous multifractals. On one hand, continuous multifractals, like fractals, have long-

range spatial correlations, but they differ from fractals by their continuity. On the other hand, multifractals are different from classical correlated media used, for example, in hydrogeology [15,16] because their correlation pattern does not have any characteristic scale outside its endmost cutoffs. The interest for these continuous multifractals is double. First, they are a typical kind of continuous structure without homogenization scale. Second, they begin to be observed in natural underground media [17–19]. Permeability distribution has been found to be multifractal in highly documented alluvial and glacial outwash aquifers on scale ranges varying from one to two orders of magnitude [17]. The fracture aperture distribution linked to the fracture permeability has also been observed to be multifractal on borehole televiewer images [19]. The understanding of the transient diffusion response is important in groundwater hydrology as it is used to extract permeability values from transient well tests [20].

The class of multifractals studied here is characterized by a continuous field and by the second-order dimension D_2 of the multifractal spectrum. D_2 basically defines the autocorrelation scaling of the multifractal measure. The generation of the multifractals is based on a multiplicative cascade process [21,22]. Diffusion is simulated numerically using the backward differentiation method [23] which proves to be efficient for stiff problems. Because of the widely scattered range of the diffusion-time scales between realizations, we calculate the anomalous diffusion exponent d_w and the fracton dimension d_s for each realization and analyze their resulting distributions. The fracton dimension characterizes the evolution with time of the probability of return to the origin $d_s = 2/d_w$ [2,24].

We found that the mean anomalous and fracton dimensions are equal to those of homogeneous media showing that, on average, the key parameter is the fractal dimension of order 0, equal to the Euclidean dimension and not to the correlation dimension D_2. Beyond their average, the exponents are highly variable between realizations. The anomalous diffusion and fracton exponents d_w and d_s range in the interval [1,4]. d_w can be consistently either larger or lower

than 2, indicating possible subdiffusive and superdiffusive regimes [25].

We show that the exponent variability is linked to the local conductivity at the medium inlet. Long-range correlations induce a broad conductivity distribution from which the conductivity at the medium inlet is drawn. Depending on the value of the conductivity at the inlet compared to the mean conductivity, diffusion samples a medium of increasing or of decreasing conductivity inducing a superdiffusive or a subdiffusive behavior. Fractal correlations ensure a regular and consistent conductivity scaling of exponent θ_0 with $\langle K(r) \rangle \sim r^{-\theta_0}$. When conditioning the simulations by the inlet conductivity, we find general relations first between the inlet conductivity and the exponent of the conductivity scaling, θ_0, and secondly between θ_0 and the anomalous diffusion exponent: $d_w(\theta_0) = (2 - D_2) + (2 - \theta_0)$. The exponents d_w and d_s depend thus on a realization characteristic, the conductivity at the medium inlet, and are only very slightly dependent on the multifractal spectrum.

In Sec. II, we describe the multifractal models and the numerical tools used for the simulation of diffusion and the exponent calculation. In Sec. III, we show the results for bidimensional continuous multifractal media and conclude on the independence of the mean exponents on the correlation dimension D_2 and the large variability of the exponents. By conditioning the simulations by the conductivity at the medium inlet, we explain the anomalous diffusion and fracton exponent variability.

II. MODEL AND METHODS

A. Characterization and generation of bidimensional continuous multifractals

A multifractal object is characterized by the infinite set of generalized dimensions D_q, with $D_0 \geqslant D_1 \geqslant D_2 \geqslant \ldots \geqslant D_\infty$, called the multifractal spectrum [14,26]. By definition, the multifractal spectrum is related to a measure (here the conductivity σ) on a support (the object itself). For the bidimensional continuous multifractal handled here, $D_0 = 2$ and D_2 define the scaling of the correlation function $C(r)$,

$$C(r) = \frac{1}{V} \int_V \sigma(r + r') \sigma(r') dV \sim r^{D_2 - d},$$

where d is the embedding Euclidean dimension.

To generate a continuous bidimensional multifractal, we have implemented a method fully described in Ref. [27] and based on a multiplicative cascade process [21,22]. The principle of the multiplicative cascade process is a recursive operation of fragmentation of a generic shape in n subdomains. Then a probability P_i, with $i = 1, \ldots, n$, is attributed to each subdomain. The fragmentation cascade can be iterated at infinity (practically set to five iterations); at each stage of the fragmentation process, a fragment takes one of the n probabilities P_i multiplied by the probability of the parent domain.

The set of probabilities P_i defines the multifractal spectrum of the generated probability field. In theory, if l is the scale ratio of the elementary fragmentation process (i.e., ratio
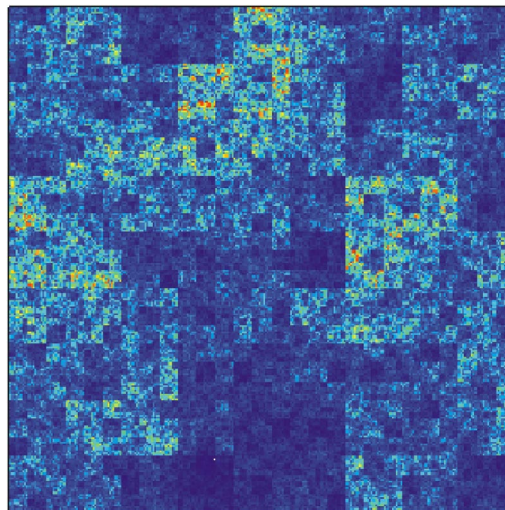

FIG. 1. (Color online) Example of a continuous multifractal of size $L = 243 l_{min}$ generated for $D_2 = 1.5$. Conductivity increases from blue to red.

between the size of the parent domain and of each fragmented subdomains, practically equal to 3 here), the dimensions D_q of the eventual probability field are related to the set $\{P_i\}_{i=1,\ldots,n}$ by [26]

$$\text{if } i \neq 1 \sum_{i=1}^{n} P_i^q = \left(\frac{1}{l}\right)^{(q-1)D_q},$$

$$\text{if } i = 1 \sum_{i=1}^{n} P_i \ln(P_i) = -D_1 \ln(l). \tag{1}$$

The method is flexible and allows generating a large range of multifractal fields.

We choose a model with a fragmentation in nine blocks of identical size [$l = 3$ in Eq. (1)] and to place the inlet at the center of the grid in order to inject the diffusion pulse at the center of the multifractal pattern. We fix the dimension D_2 [$q = 2$ in Eq. (1)] as the main characteristic of the generated probability field, but we let the other dimensions D_1 and $\{D_q\}_{q>2}$ undetermined, which means that they can take whatever value between 1 and 2. Also we choose an isotropic fragmentation process, meaning that the probabilities $\{P_i\}_{i=1,\ldots,9}$ are randomly permuted before being mapped on the subdomains.

In practice, the multiplicative cascade process is iterated four or five times so that the multifractal structure is defined from a minimal scale l_{min} set equal to the unit reference and equal to the mesh size, up to the medium size equal to $L = 81 l_{min} = 3^4 l_{min}$ or $L = 249 l_{min} = 3^5 l_{min}$ (Fig. 1). Note that below the mesh scale l_{min}, the medium is homogeneous. The conductivity K is obtained from the probability P by a simple multiplication by $(L/l_{min})^2 K_{unit}$, where K_{unit} is the unit conductivity. As $\Sigma P = 1$, $\langle K \rangle$ remains equal to K_{unit} whatever the system size L.
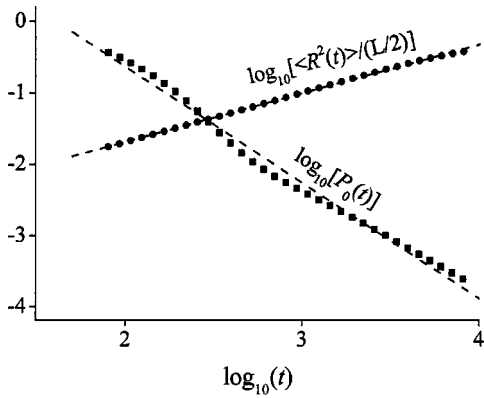
FIG. 2. Example of a grid for which have been calculated the radius of diffusion $R^2(t)$ normalized by half of the system size $L/2$ and the probability density $P_0(t)$ at the grid inlet. The dashed lines represent the best linear fits which give: $\theta = -0.9$, $d_w = 1.5$, and $d_s = 3.2$. Oscillations in $P_0(t)$ are a realization effect and have not been systematically observed.

B. Simulation of diffusion

The classical diffusion equation $\partial P/\partial t = \nabla(K\nabla P)$ with $P(r,t)$ the unknown was discretized on the grid with a finite volume method using a two-steps centered scheme in space and a multistep scheme in time. The advantage of the numerical scheme over exact enumeration and random-walk techniques [2] relies on the possibility of dealing with media having a broad-range distribution of conductivity. The intermesh conductivity was taken as the harmonic mean of the neighboring mesh conductivities [28]. The widely scattered heterogeneity produces a stiff numerical problem for which multistep schemes like the backward differentiation formula are well suited [29]. We have chosen to use the free package called LSODE [23], which implements an implicit BDF scheme. It has a number of features which guarantee efficiency and accuracy, such as a varying order (from 1 to 5), an adaptive step size, and a sparse linear solver. Solving on a grid of size $L = 243 l_{\min}$ takes around half an hour on a personal workstation. For each set of parameters, Monte Carlo simulations are made up of at least 100 grids.

C. Computation of the anomalous diffusion and fracton exponents d_w and d_s

The exponents d_w and d_s are defined by the scaling of the mean square radius of diffusion $\langle R^2(t)\rangle = t^{2/d_w}$ and the probability at the grid inlet $P_0(t) = t^{-d_s/2}$ for a pulse injected at the medium center [2]. Exponents are classically obtained on $\langle R^2(t)\rangle$ and $P_0(t)$ by Monté Carlo simulations.

In the case of continuous multifractals treated here, the exploitable time scale ranges from the time at which the pulse leaves the inlet mesh t_{in} to the time at which the diffused pulse leaves the gird t_{out}. Practically, t_{in} and t_{out} have been defined, respectively, as the time for which the radius of diffusion is equal to the mesh size and as the time at which 2% of the diffused pulse has left the system. Between realizations and because of different conductivity ranges, the exploitable time range $\log_{10}(t_{\text{out}}/t_{\text{in}})$ is highly variable between
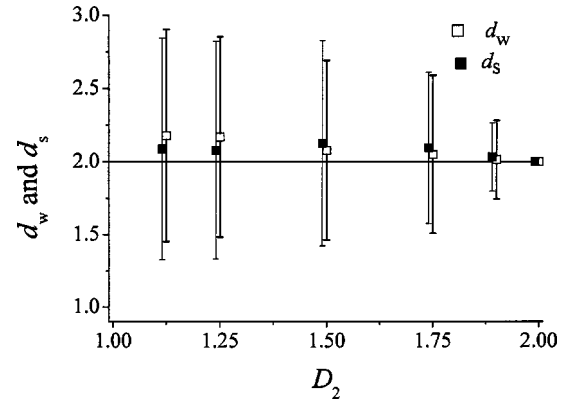

FIG. 3. d_w and d_s as functions of D_2. The statistics were derived from 660 realizations for each value of D_2. The horizontal line characterizes normal transport ($d_w = d_s = 2$).

2 and 4 for grids of size $L = 243 l_{\min}$. The resultant radius of diffusion and inlet probability cannot thus be averaged. Alternatively, we have derived the exponents directly on each realization, and studied their statistics over different realizations. We have validated this method on off-lattice percolation clusters at threshold in two dimensions of size $L = 75 l_{\min}$ and found $d_w = 2.96 \pm 0.2$ and $d_s = 1.38 \pm 0.2$, which are close to the known values $d_w = 2.86$ and $d_s = 1.326$ [7]. The large error ranges come from the fitting on $2/d_w$ and on $d_s/2$. To have a more precise knowledge of the fitting quality, we have looked at the chi-square values χ^2 of the fits. Values of χ^2 are in the range $[0.002;0.06]$ and $[0.02;0.1]$ for $\langle R^2(t)\rangle$ and $P_0(t)$, respectively. Examples of fits with χ^2 equal to 0.003 and 0.04 for $\langle R^2(t)\rangle$ and $P_0(t)$ are given by Fig. 2. In the following, d_w and d_s are average exponents obtained on at least 100 grids.

III. RESULTS

A. Exponents d_w and d_s as functions of the correlation dimension D_2

Results of the simulation of diffusion in grids of size $L = 243 l_{\min}$ (Fig. 1) show that d_w and d_s are on average very
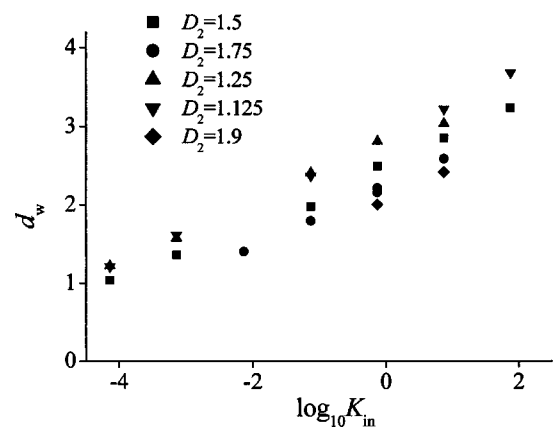

FIG. 4. Average values of d_w obtained on 100 realizations as a function of the inlet conductivity K_{in}.
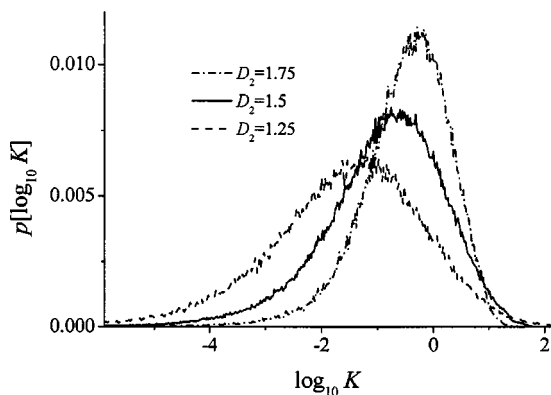
FIG. 5. Distribution of the logarithm of conductivity.

close to 2 whatever the correlation dimension D_2 (Fig. 3). On average, the dimensions obtained on continuous multifractals are those of the homogeneous medium. The same result was found for continuous different long-range correlated media generated with a fractional Brownian motion characterized by the Hurst coefficient H and having a correlation dimension $D_2=2+2H$ with H in [0,1] [13]. However, the average does not describe fully the exponent distributions as the exponents are highly variable between realizations. The anomalous diffusion and fracton exponents d_w and d_s range in the interval [1,3] indicating possible subdiffusive and superdiffusive regimes for d_w, respectively, larger and lower than 2 [25]. The absence of influence of D_2 shows that the exponents d_w and d_s are not function of the dimension of correlation D_2. Are they connected to another medium characteristic?

B. Exponents d_w and d_s as functions of the inlet conductivity

We have calculated the anomalous diffusion exponent d_w as a function of the conductivity at the grid inlet K_{in}. Results given by Fig. 4 show a very good correlation between K_{in} and d_w and more precisely a systematic increase of d_w from around 1 to 3 whatever the correlation dimension D_2 and only slightly sensitive to D_2. The following paragraphs are dedicated to explain and quantify this correlation. We argue that the conductivity regularly increases or decreases from
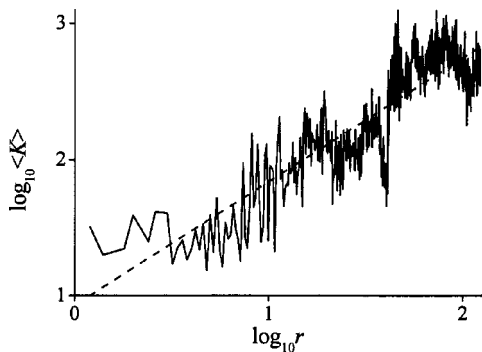

FIG. 6. Example of a grid for which has been calculated the conductivity scaling against the radius from the inlet. The dashed line is the best linear fit on the log-log data.
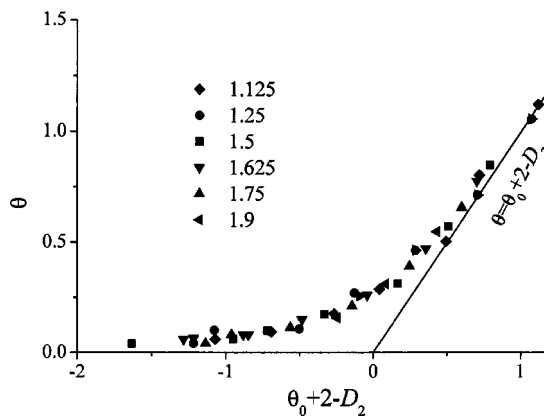

FIG. 7. Relation between θ and θ_0.

the conductivity inlet K_{in} to the large-scale average conductivity inducing, respectively, a speed up or a slow down of diffusion. We will show, first, how conductivity evolves with scale and, second, how the conductivity scaling and the anomalous diffusion exponent d_w are related.

1. Relation between the inlet conductivity K_{in} and the conductivity scaling exponent θ_0

The multifractal conductivity pattern has two key characteristics: it is correlated over all scales and it has a large distribution of conductivities. In fact the conductivity distribution spans several orders of magnitude as shown in Fig. 5. The conductivity at the inlet of the grid is randomly drawn from this conductivity distribution whereas the large-scale conductivity is on average equal to the unit conductivity K_{unit} according to the generation procedure. Conductivity can thus increase or decrease from its value at the grid inlet to its large-scale averaged value. To quantify the conductivity scaling, we have computed the mean conductivity $\langle K \rangle$ on rings of evolving radii r (Fig. 6). The multifractal nature of the correlation pattern warrants the regular and consistent evolution of $\langle K \rangle$ with scale such as $\langle K(r) \rangle \sim r^{-\theta_0}$. Knowing that $\langle K \rangle$
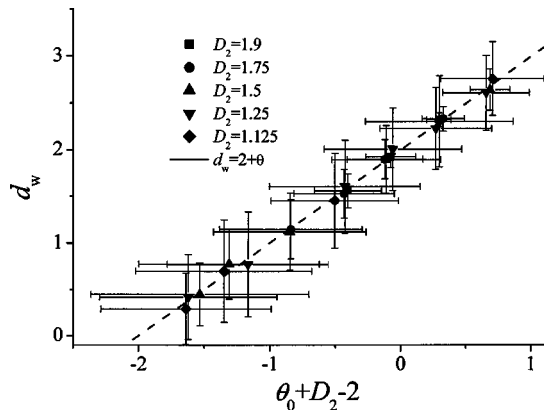

FIG. 8. d_w function of θ_0+D_2-2 where θ_0 is defined by $\langle K(r) \rangle \sim r^{-\theta_0}$. The line $d_w=2-\theta_0+D_2-2$ is the theoretical prediction of Ref. [4].
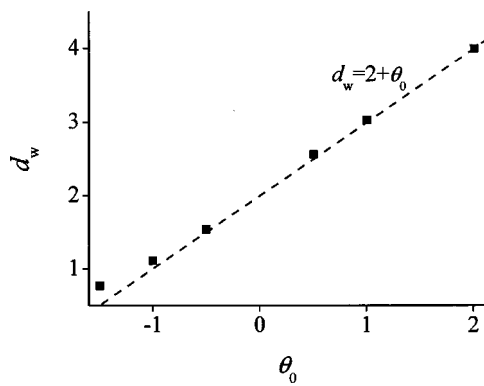
FIG. 9. d_w function of θ_0 for annular media whose conductivity is defined by $K(r)=r^{-\theta_0}$.

FIG. 10. d_s function of d_w for different values of the conductivity at the system inlet K_{in}. The dashed line $d_s/2=2/d_w$ comes from Ref. [4] with a fractal dimension equal to the Euclidean dimension 2.

is equal to K_{in} at the system inlet and to K_{unit} at the system size, the exponent θ_0 is given by

$$\theta_0 = -\frac{\log_{10} K_{unit} - \log_{10} K_{in}}{\log_{10} L - \log_{10} l_{min}} \qquad (2)$$

whatever the correlation dimension D_2, which is confirmed by numerical simulations. Note that we verified on D_1 [defined by Eq. (1)] that the conditioning by the inlet conductivity K_{in} does not fix the other multifractal dimensions.

2. Relation between the conductivity scaling exponent θ_0 and the anomalous diffusion and fracton exponents d_w and d_s

The conductivity increase or decrease characterized by θ_0 is a sampling effect of the conductivity distribution that induces, respectively, a speed up or a slow down of diffusion characterized by d_w. On the percolating cluster at threshold as well as on the Sierpinski gasket, the fractal structure induces a decrease of the equivalent conductivity $\hat{K}(r)$ with scale characterized by the exponent $-\theta(\hat{K}(r)\sim r^{-\theta})$ and an anomalously slow diffusion of exponent d_w [1,4]. Both exponents are related by

$$d_w = 2 + \theta \qquad (3)$$

with $\theta=0.878$ for the percolation cluster at threshold [30] and $\theta=0.32$ for the Sierpinski gasket [4]. The equivalent conductivity $\hat{K}(r)$ is derived from the total integral resistance derived in radial flow conditions (by the equivalence between the electrical conductivity and diffusion problems) [4]. According to this definition, θ integrates the flow conditions within the medium whereas θ_0 is a simple geometrical average. For continuous multifractals, numerical simulations show first that θ and θ_0 are simply related when K decreases with scale ($\theta_0>0$) (Fig. 7)

$$\theta = \theta_0 + D_2 - 2 \qquad (4)$$

and secondly that the relation established for the Sierpinski gasket $d_w=2+\theta$ still holds (Fig. 8). When K increases with scale ($\theta_0<0$), the equivalent conductivity like an in-series system is dominated by the lowest conductivity which is the
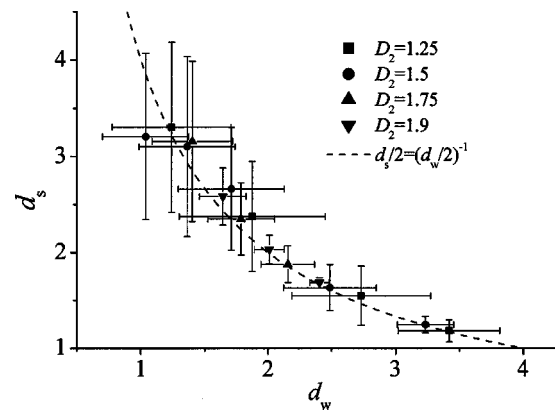
conductivity at the origin. θ remains slightly larger than 0 (Fig. 7) and the relation (3) is no longer verified. However, d_w remains related to θ_0 in the same way as for $\theta_0>0$ (Fig. 8).

We have numerically verified that the relation $d_w=2+\theta$ is also relevant to "homogeneous" annular media whose conductivity is defined by $K(r)=r^{-\theta_0}$ and $\theta=\theta_0$ (Fig. 9). For "heterogeneous" media having the same conductivity scaling on average $\langle K(r)\rangle\sim r^{-\theta_0}$, diffusion is slower for smaller values of D_2 with $d_w=2+\theta_0+2-D_2$. Heterogeneity induces thus a slower diffusion quantified by an increase of the exponent d_w by $2-D_2$.

The validity of the framework established for the Sierpinski gasket [4] is enhanced by the relation between the fracton and anomalous diffusion exponents d_s and d_w obtained for a fractal dimension equal to 2 (Fig. 10):

$$d_s/2 = 2/d_w. \qquad (5)$$

IV. CONCLUSION

The anomalous diffusion and fracton exponents when averaged over all possible configurations are not function of the correlation dimension. However, beyond the average, the exponent range is very large and extends practically from 1 to 4. The large exponent variability can be explained by a local property: the conductivity at the grid inlet. In fact the multifractal correlation and the large conductivity distribution create a conductivity upscaling or down-scaling from the inlet conductivity K_{in} to the large-scale average conductivity K_{unit}. The resulting conductivity scaling induces an anomalous diffusion of exponent d_w given from Eqs. (2) and (3) by

$$d_w(K_{in}) = 4 - D_2 - \frac{\log_{10}(K_{unit}/K_{in})}{\log_{10}(l_{min}/L)},$$

where l_{min} and L are the mesh and grid sizes. The fracton dimension d_s remains linked to the anomalous diffusion exponent d_w by the classical relation (5).

[1] Y. Gefen, A. Aharony, and S. Alexander, Phys. Rev. Lett. **50**, 77 (1983).

[2] S. Halvin and D. Ben-Avraham, Adv. Phys. **36**, 695 (1987).

[3] J.-P. Bouchaud and A. Georges, Phys. Rep. **195**, 127 (1990).

[4] B. O'Shaughnessy and I. Procaccia, Phys. Rev. A **32**, 3073 (1985).

[5] J. Klafter, G. Zumofen, and A. Blumen, J. Phys. A **20**, 4835 (1991).

[6] R. A. Guyer, Phys. Rev. A **29**, 2751 (1984).

[7] D. Stauffer and A. Aharony, *Introduction to Percolation Theory*, 2nd ed. (Taylor and Francis, Bristol, 1992).

[8] S. Prakash *et al.*, Phys. Rev. A **46**, R1724 (1992).

[9] M. Sahimi and S. Mukhopadhyay, Phys. Rev. E **54**, 3870 (1996).

[10] A. Weinrib, Phys. Rev. B **29**, 387 (1984).

[11] S. Feng, B. I. Halperin, and P. N. Sen, Phys. Rev. B **35**, 197 (1987).

[12] E. Charlaix, E. Guyon, and S. Roux, Transp. Porous Media **2**, 31 (1987).

[13] M. Saadatfar and M. Sahimi, Phys. Rev. E **65**, 036116 (2002).

[14] H. G. E. Hentschel and I. Proccacia, Physica D **8**, 435 (1983).

[15] L. W. Gelhar, *Stochastic Subsurface Hydrology* (Engelwood Cliffs, New Jersey, 1993).

[16] G. Dagan, *Flow and Transport in Porous Formations* (Springer-Verlag, Berlin, 1989).

[17] L. Tennekoon *et al.*, Water Resour. Res. **39**, 1193 (2003).

[18] M. C. Boufadel *et al.*, Water Resour. Res. **36**, 3211 (2000).

[19] W. C. Belfield, Geophys. Res. Lett. **21**, 2641 (1994).

[20] G. de Marsily, *Quantitative Hydrogeology: Groundwater Hydrology for Engineers* (Academic Press, Orlando, FL, 1986).

[21] D. Schertzer and S. Lovejoy, J. Geophys. Res., [Atmos.] **92**, 9693 (1987).

[22] P. Meakin, Physica A **173**, 305 (1991).

[23] A. C. Hindmarsh, *in Scientific Computing*, edited by R. S.*et al.* (IMACS/North-Holland, Amsterdam, 1983), p. 55.

[24] S. Alexander and R. Orbach, J. Phys. (Paris), Lett. **43**, L625 (1982).

[25] R. Metzler and J. Klafter, Phys. Rep. **339**, 1 (2000).

[26] J. Feder, *Fractals* (Plenum Press, New York, 1988).

[27] C. Darcel *et al.*, Water Resour. Res. **39**, 1272 (2003).

[28] R. Kruel-Romeu and B. Noetinger, Water Resour. Res. **31**, 943 (1995).

[29] E. Hairer and G. Wanner, *Solving Ordinary Differential Equations II. Stiff and Differential-Algebraic Problems* (Springer-Verlag, Berlin, 1991).

[30] P. Grassberger, Physica A **262**, 251 (1999).